J Solid State Electrochem (2010) 14:2285–2292
DOI 10.1007/s10008-010-1060-6

ORIGINAL PAPER

Nanomolar determination of hydrazine by TiO_2 nanoparticles modified carbon paste electrode

M. Mazloum-Ardakani · H. Rajabi · B. B. F. Mirjalili · H. Beitollahi · A. Akbari

Received: 29 January 2010 / Revised: 15 March 2010 / Accepted: 21 March 2010 / Published online: 21 April 2010

Abstract In the present paper, the use of a novel carbon paste electrode modified by *N*,*N*′(2,3-dihydroxybenzylidene)-1,4-phenylene diamine (DHBPD) and TiO_2 nanoparticles prepared by a simple and rapid method for the determination of hydrazine (HZ) was described. In the first part of the work, cyclic voltammetry was used to investigate the redox properties of this modified electrode at various solution pH values and at various scan rates. A linear segment was found with a slope value of about 48 mV/pH in the pH range 2.0–12.0. The apparent charge transfer rate constant (k_s) and transfer coefficient (α) for electron transfer between DHBPD and TiO_2 nanoparticles-modified carbon paste electrode were calculated. In the second part of the work, the mediated oxidation of HZ at the modified electrode was described. It has been found that under optimum condition (pH 8.0) in cyclic voltammetry, a high decrease in overpotential occurs for oxidation of HZ at the modified electrode. The values of electron transfer coefficients (α) and diffusion coefficient (D) were calculated for HZ, using electrochemical approaches. Differential pulse voltammetry exhibited a linear dynamic range from 1.0×10^{-8} to 4.0×10^{-6} M and a detection limit (3σ) of 9.15 nM for HZ. Finally, this method was used for the determination of HZ in water samples, using standard addition method.

Keywords Hydrazine · TiO_2 nanoparticles · Modified carbon paste electrode · Electrocatalysis

M. Mazloum-Ardakani (✉) · H. Rajabi · B. B. F. Mirjalili · H. Beitollahi · A. Akbari
Department of Chemistry, Faculty of Science, Yazd University, Yazd 89195-741 IR, Iran
e-mail: mazloum@yazduni.ac.ir

Introduction

Electroanalysis is one of the best methods for detecting species in a solution due to its low cost, ease of use, and reliability [1]. Most developments in electroanalytical chemistry in recent years have originated from advances in sensor design, chemical modification, and functionalization of electrodes for enhanced sensitivity and selectivity of electroanalysis [2, 3].

Nanomaterials have added a new dimension to electroanalysis and electrode development. The unique properties of these materials have led to simple and highly sensitive electroanalytical procedures that could not be accomplished by standard electrochemical methods. Nanomaterials have brought four main advantages to a modified electrode when compared to a microelectrode; among them are high effective surface area, mass transport, catalysis, and control over local microenvironment [4]. A broad range of nanomaterials especially nanotubes and nanoparticles with different properties have found wide applications in many analytical methods [5].

Hydrazine (HZ) and its derivatives are widely used in agricultural chemicals (pesticides), chemical blowing agents, pharmaceutical intermediates, photography chemicals, and boiler water treatment in hot-water heating systems for corrosion control [6]. It is also employed as a starting material for many derivatives such as foaming agents for plastics, antioxidants, polymers, and plant-growth regulators. Moreover, HZ, its salts, and its methyl and dimethyl derivatives are used as rocket fuel, gas generators, and explosives [7, 8]. HZ and its derivatives are industrial chemicals that enter the environment primarily by emissions from their uses as aerospace fuels and from industrial facilities that manufacture, process, or use these chemicals. HZ is volatile and toxic and is readily

absorbed by oral, dermal, or inhalation routes of exposure [9]. Acute exposure can also damage the liver, the kidneys, and the central nervous system in humans [8, 10, 11]. The carcinogenic risks to humans of HZ and its derivatives have been considered on a number of occasions by the International Agency for Research on Cancer of the World Health Organization [12, 13]. Environmental Protection Agency (EPA) has classified HZ as a group B_2 (human carcinogen) [10].

EPA and the Agency for Toxic Substance and Disease Registry calculated an intermediate inhalation minimal risk level of 0.004 μg ml^{-1} [10, 14]. The National Institute for Occupational Safety and Health and the Occupational Safety and Health Administration recommended that the level of HZ in workplace air should not exceed 0.03 μg ml^{-1} for a 2-h period [15, 16]. Furthermore, the Food and Drug Administration has ruled that HZ cannot be added to water used for making steam that will contact food. Because of the environmental and toxicological significance of HZ compounds, sensitive and reliable analytical methods are necessary for preconcentration and determination of HZ in samples.

Several instrumental methods for determination of HZ by amprometry [17], differential pulse voltammetry [18], chromatography [19], spectrophotometry [20], flow injection with spectrophotometry [21] and fluorimetry [22] have been reported.

The direct oxidation of HZ has been studied at several electrodes including mercury, silver, gold, platinum, and nickel. Although metals such as Pt, Au, and Ag are very active in the anodic oxidation of HZ, they are too expensive for practical applications and require a large overpotential for HZ determination.

A major attention has been focused on the development of chemically modified electrodes during the last two decades. They exploit the ability of certain surface-bound redox mediators to enhance electron-transfer kinetics and thus lower the operating potential. Hence, relatively large amounts of electrochemical research have been devoted to the development and application of different types of chemically modified electrodes [23, 24]. Thus, a wide variety of compounds has been used as electron transfer mediators for the anodic oxidation of HZ [25–39].

To the best of our knowledge, no study has been published so far on the electrocatalytic oxidation of HZ by using *N*,*N*′(2,3-dihydroxybenzylidene)-1,4-phenylene diamine (DHBPD)–TiO_2 nanoparticles-modified carbon paste electrode (DHBPDTNMCPE). Thus, in the present work, we described initially the preparation and suitability of a DHBPDTNMCPE as a new electrode in the electrocatalysis and determination of HZ in an aqueous buffer solution. Then, in order to demonstrate the capability of the modified electrode in the electrooxidation of HZ in real samples, we examined this method for the voltammetric determination of HZ in water samples.

Experimental

Apparatus and chemicals

The electrochemical measurements were performed with a potentiostat/galvanostat (SAMA 500, electroanalyzer system, IR, Iran). A conventional three-electrode cell was used at 25±1°C. A saturated calomel electrode, a platinum wire, and DHBPDTNMCPE were used as reference, auxiliary, and working electrodes, respectively. A Metrohm model 691-pH/mV meter was also used for pH measurements.

All solutions were freshly prepared with doubly distilled water. HZ and other reagents were analytical grade (Merck, Darmstadt, Germany). Graphite powder (Merck) and paraffin oil (DC 350, Merck, density=0.88 g cm^{-3}) were used as binding agents for graphite pastes. Buffer solutions were prepared from orthophosphoric acid and its salts in the pH range of 2.0–12.0.

Preparation of TiO_2 nanoparticles

Colloidal suspension of TiO_2 nanoparticles was synthesized by mixing titanium tetraisopropoxide, H_2O_2, and H_2O with volume proportions of 12:90:200, respectively. The resulting solution was refluxed for 10 h to promote the crystallinity (surface area=84 m^2 g^{-1} and particle size=6.7 nm).

Typical procedure for preparation of DHBPD in the presence of 37% $BF_3.SiO_2$

A mixture of 2,3-dihydroxybenzaldehyde (0.276 g, 2 mmol), benzene-1,4-diamine (0.108 g, 1 mmol), and 37% $BF_3.SiO_2$ (0.300 g) was heated with stirring at 80 °C for 15 min in $CHCl_3$ (5 ml). After completion of reaction, the product was dissolved to $CHCl_3$ (5 mL) and filtered to recover the catalyst. The solvent was evaporated and the crude product was recrystallized from methanol compound. It was obtained as red crystals at ~ 93.2% yield. The structure of product was fully characterized by IR and ^1H NMR spectroscopy IR (KBr, cm^{-1}): 3,100–3,300 (b, OH), 1,618(C=N), 1,407, 1,506(Ar, C=C), 1,250(C–O), 1,218, 1,159, 834, 789, 500 ^1H NMR(DMSO–D_6, 400MHz)/δ ppm: 6.72(t, 2H,), 6.91(d, 2H), 6.98(d, 2H), 7.39(s, 4H), 7.95(s, 1H), 8.7(s, 2H).

Preparation of the electrode

DHBPDTNMCPE was prepared by dissolving 0.01 g of DHBPD in CH_3Cl and hand mixing with 95 times its

weight of graphite powder and four times its weight of TiO_2 nanoparticles using a mortar and pestle. Paraffin was added to the above mixture and mixed for 20 min until a uniformly wetted paste was obtained. This paste was then packed into the end of a glass tube (ca. 3.35 mm intradermally and 10 cm long). A copper wire inserted into the carbon paste provided an electrical contact. When necessary, a new surface was obtained by pushing an excess of paste out of the tube, which was then polished with weighing paper. DHBPD-modified CPE (DHBPDMCPE) and TiO_2 nanoparticle CPE (TNCPE) were prepared in the same way without adding TiO_2 nanoparticles and DHBPD, respectively. In addition, unmodified CPE was prepared in the same way without adding DHBPD and TiO_2 nanoparticles to the mixture. These were used for the purpose of comparison.

Results and discussion

Electrochemical properties of DHBPDTNMCPE

Based on our knowledge, there has not been prior report of a study on the electrochemical properties and, in particular, the electrocatalytic activity of DHBPDTNMCPE in aqueous media. This compound is insoluble in aqueous media; therefore, we prepared DHBPDTNMCPE and studied its electrochemical properties in a buffered aqueous solution (pH 8.0) using cyclic voltammetry. Experimental results show well-defined and reproducible anodic and cathodic peaks (with E_{pa}=0.26 V, E_{pc}=0.12 V, $E^{\circ\prime}$=0.19 V versus SCE and ΔE_p=0.14 V) for DHBPD; therefore, this substance can be used as mediator for the electrocatalysis of some important biological compounds with slow electron transfer.

As shown, the peak separation potential, $\Delta E_p=(E_{pa}-E_{pc})$ was greater than the $59/n$ mV expected for a reversible system, indicating that the redox couple of DHBPDTNMCPE behaves quasireversible in the buffered aqueous solution.

In addition, the effect of the potential scan rate on electrochemical properties of the DHBPDTNMCPE was studied in an aqueous solution with cyclic voltammetry (Fig. 1). Plots of the anodic and cathodic peak currents (I_p) were linearly dependent on ν at scan rates from 10 to 1,000 mV s^{-1}. A linear correlation was obtained between peak currents, and the scan rate indicates that the nature of redox process was controlled in a diffusionless manner (Fig. 1a).

The apparent charge transfer rate constant (k_s) and the charge transfer coefficient (α) of a surface-confined redox couple can be evaluated from cyclic voltammetric experiments and by using the variation of anodic and cathodic peak potentials with logarithm of scan rate, according to the procedure of Laviron [40]. Figure 1b shows the variations of peak potentials (E_p) as a function of the logarithm of the potential scan rate. We found that the E_p values are proportional to the logarithm of the potential scan rate, for scan rates higher than 1,000 mV s^{-1} (Fig. 1b). The slopes of Fig. 1b plot can be used to extract the kinetic parameters α_a (anodic transfer coefficient). The slope of the linear segment is equal to $2.303RT/(1-\alpha)nF$ for the anodic peaks. The evaluated value for the anodic transfer coefficient (α_a) is 0.44.

In addition, the following equation can be used to determine the electron transfer rate constant between modifier (DHBPD) and CPE:

$$\log k_s = \alpha \log(1-\alpha) + (1-\alpha) \log \alpha - \log(RT/nF\nu) - \alpha(1-\alpha) nF\Delta E_p/2.3RT \quad (1)$$

where $(1-\alpha)n_\alpha$=0.56, ν is the sweep rate, and all other symbols having their conventional meanings. The value of k_s=2.36±0.13 s^{-1} was evaluated using Eq. 1.

Influence of pH

The electrochemical response of the DHBPD molecule is generally pH dependent. Thus, the electrochemical behavior of the DHBPDTNMCPE was studied at different pHs using differential pulse voltammetry. Anodic peak potentials of the DHBPDTNMCPE were shifted to less positive values with increases in pH. A potential-pH diagram was constructed by plotting the E_p values as a function of pH (Fig. 1c). This diagram is composed of a straight line with slope=48 mV/pH. Such behavior suggests that it obeys the Nernst equation for a two electron and proton transfer reaction [41].

Electrocatalytic oxidation of HZ at a DHBPDTNMCPE

Figure 2 depicts the cyclic voltammetric responses from the electrochemical oxidation of 0.1-mM HZ at the unmodified CPE (curve a), TiO_2 nanoparticle CPE (TNCPE) (curve b), DHBPDMCPE (curve c), and DHBPDTNMCPE (curve d). As shown, at the DHBPDMCPE (curve c) and the DHBPDTNMCPE (curve d), the peak potential was about 260 mV, while at the unmodified CPE (curve a) and the TNCPE (curve b), HZ is not oxidized until 750 mV. Thus, a decrease in overpotential for hydrazine is achieved with the modified electrode. This value is comparable to values reported by other researchers for the electrocatalytic oxidation of HZ at the surface of chemically modified electrodes by other mediators previously (Table 1).

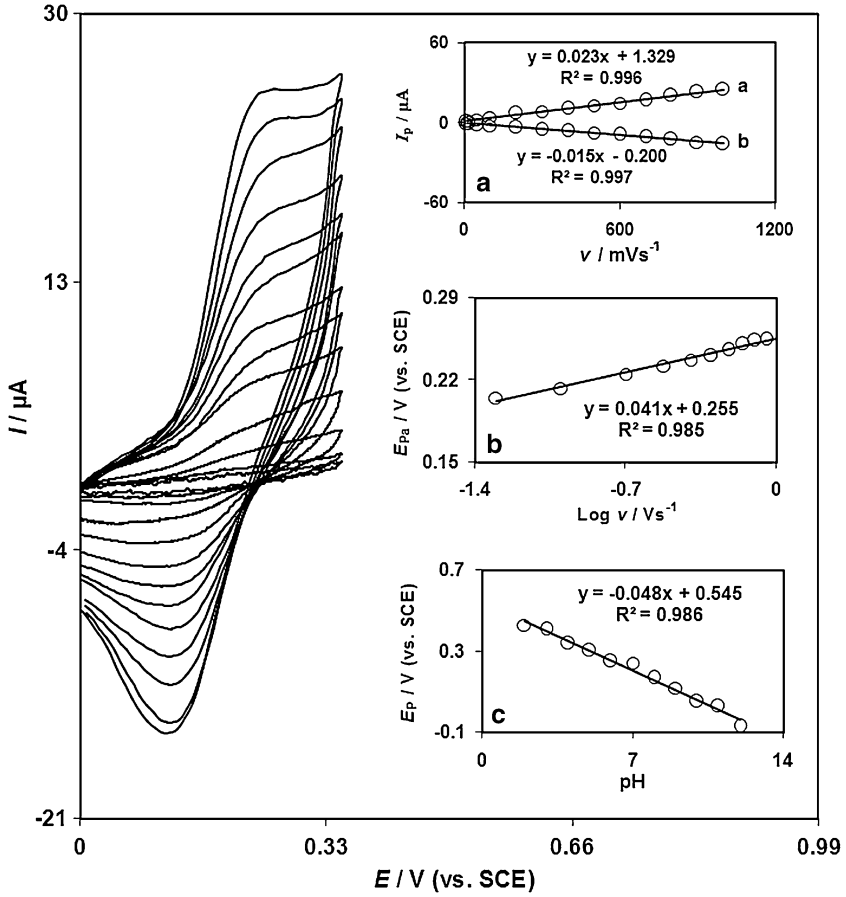

Fig. 1 Cyclic voltammograms of DHBPDTNMCPE in a 0.1-M phosphate-buffered solution (PBS, pH 8.0), at various scan rates, from inner to outer correspond to 10, 20, 50, 100, 200, 300, 400, 500, 600, 700, 800, 900, and 1,000 mV s^{-1} scan rates. **a** Variations of I_p versus scan rates. **b** Variation of E_p versus the logarithm of the scan rate. **c** Plot of anodic potential peak (E_{Pa}) of DHBPDTNMCPE versus various pHs: 2.0, 3.0, 4.0, 5.0, 6.0, 7.0, 8.0, 9.0, 10.0, 11.0, and 12.0

Similarly, when comparing the oxidation of HZ at the DHBPDMCPE (curve c) and the DHBPDTNMCPE (curve d), enhancement of the anodic peak current at the BBNBHTNMCPE relative to that obtained at the DHBPDMCPE was observed. In other words, the data clearly show that the combination of TiO_2 nanoparticles and mediator (DHBPD) definitely improve the characteristics of HZ oxidation.

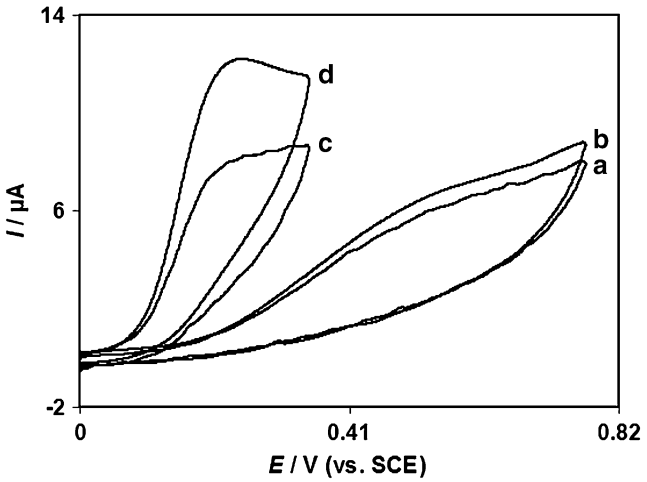

Fig. 2 Cyclic voltammograms of **a** CPE, **b** TNCPE, **c** DHBPDMCPE, and **d** DHBPDTNMCPE in 0.1-M PBS (pH 8.0) containing 0.1-mM HZ at scan rate 20 mV s^{-1}

The DHBPDTNMCPE, in 0.1-M phosphate buffer (pH 8.0) at the scan rate 20 mV s^{-1} and without HZ in solution, exhibited a well-behaved redox reaction (as shown in Fig. 1) and with addition of 0.1-mM HZ, increased the anodic peak current (Fig. 2 curve d), indicating a strong electrocatalytic effect [41]. Based on these results, catalytic Scheme 1 (EC' catalytic mechanism) describes the voltammetric response of electrochemical oxidation of HZ at the DHBPDTNMCPE.

The effect of scan rate on the electrocatalytic oxidation of HZ at the DHBPDTNMCPE was investigated by cyclic voltammetry. The plot of peak height (I_p) versus the square root of scan rate ($\nu^{1/2}$), in the range of 2–40 mV s^{-1}, was constructed (Fig. 3). This plot was found to be linear, suggesting that at sufficient overpotential, the process was diffusion rather than surface controlled. A plot of the sweep rate normalized current ($I_p/\nu^{1/2}$) versus sweep rate (Fig. 3a) exhibits the characteristic shape typical of an EC′ process [41].

Table 1 Comparison of the efficiency of some modified electrodes used in the electrocatalysis of HZ

Elec.	pH	ΔE / mV	ν/ mVs^{-1}	LOD (M)	LDR (M)	D (cm^2 s^{-1})	α	$k_{catalytic}$ (M^{-1} s^{-1})	Ref.
Carbon ceramic	7.0	260	50	1×10^{-6}	6×10^{-6}–1.2×10^{-3}	5.6×10^{-6}	0.48	7.1×10^{3}	25
Carbon nanotube paste	13	–	100	8.0×10^{-7}	2.5×10^{-6}–2.0×10^{-4}	3.58×10^{-5}	–	4.78×10^{4}	26
Carbon ceramic	7.0	280	10	8×10^{-6}	2×10^{-5}–2×10^{-3}	6.28×10-^{6}	0.741	–	27
Glassy carbon	8.0	420	25	1.4×10^{-6}	2×10^{-6}–4.4×10^{-5}	2.45×10^{-6}	0.55	6.26×10^{3}	28
Glassy carbon	13	400	20	3.1×10^{-8}	2.5×10^{-7}–2.5×10^{-4}	–	–	–	29
Graphite	7.0	500	50	1.0×10^{-6}	2.4×10^{-6}–8.2×10^{-3}	–	0.721	–	30
Carbon paste	7.5	228	10	1×10^{-5}	1×10^{-5}–1×10^{-3}	–	–	–	31
Glassy carbon	9.0	–	20	5.0×10^{-7}	2.0×10^{-6}–20.0×10^{-5}	5.9×10^{-6}	0.37	2.0×10^{4}	32
Glassy carbon	7.0	515	50	2.0×10^{-7}	1×10^{-6}–7.5×10^{-3}	2.5×10^{-5}	0.52		33
Carbon paste	7.0	300	20	–	1.0×10^{-4}–1.2×10^{-2}	6.28×10^{-6}	0.4	–	34
Carbon paste	10	550	10	5.2×10^{-6}	7.0×10^{-6}–8.0×10^{-4}	2.2×10^{-6}	–	–	35
Carbon ceramic	7.0	500	20	3.0×10^{-6}	7.0×10^{-6}–1.1×10^{-3}	2.91×10^{-6}	0.55	3.2×10^{3}	36
Graphite–wax composite	7.0	450	20	6.65×10^{-6}	3.33×10^{-5}–8.18×10^{-3}	–	–	–	37
Glassy carbon	7.0	–	–	1.7×10^{-7}	5.0×10^{-7}–2.0×10^{-5}	3.4×10^{-6}	0.57	6.26×10^{3}	38
Glassy carbon	2.0	–	10	1.4×10^{-7}	2.0×10^{-7}–1.0×10^{-5}	1.1×10^{-6}	0.35	4.83×10^{3}	39
Carbon-TiO_2 nanoparticle	8.0	–	20	9.15×10^{-9}	1.0×10^{-8}–4.0×10^{-6}	5.81×10^{-6}	0.63	3.65×10^{3}	This work

Tafel plot was drawn from data of the rising part of the current–voltage curve recorded at a scan rate of 20 mV s^{-1}. This part of voltammogram, known as Tafel region, is affected by electron transfer kinetics between substrate (HZ) and surface-confined DHBPD. In this condition, the number of electron involved in the rate-determining step can be estimated from the slope of Tafel plot. A slope of 0.164 V per decade is obtained, and assuming one electron transfer to be rate limiting, a transfer coefficient (α) of 0.63 was calculated. This value is comparable to values reported by other researchers for the electrocatalytic oxidation of HZ at the surface of chemically modified electrodes by other mediators previously (Table 1).

Chronoamperometric and chronocoloumetric measurements

The chronoamperometry as well as the other electrochemical methods was also employed for the investigation of electrode processes at chemically modified electrodes. Chronoamperometric measurements of HZ at DHBPDTNMCPE were done by setting the working electrode potential at 350 mV for various concentrations of HZ. For an electroactive material (HZ in this case) with a diffusion coefficient of D, the current for the electrochemical reaction (at a mass transport-limited rate) is described by the Cottrell equation [41]. Under diffusion control, a plot of I versus $t^{-1/2}$ will be linear, and from the slope, the value of D can be obtained. Figure 4 shows the experimental plots with the best fits for different

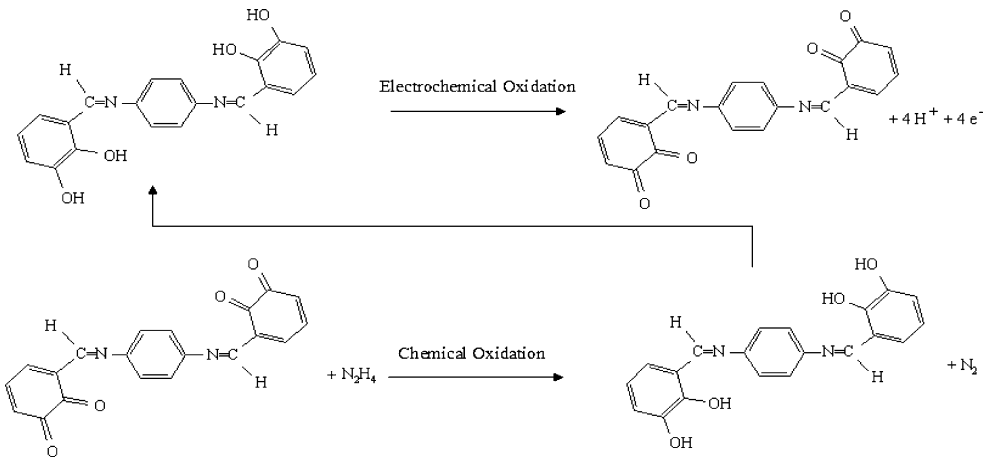

Scheme 1 EC' mechanism of HZ at the DHBPDTNMCPE

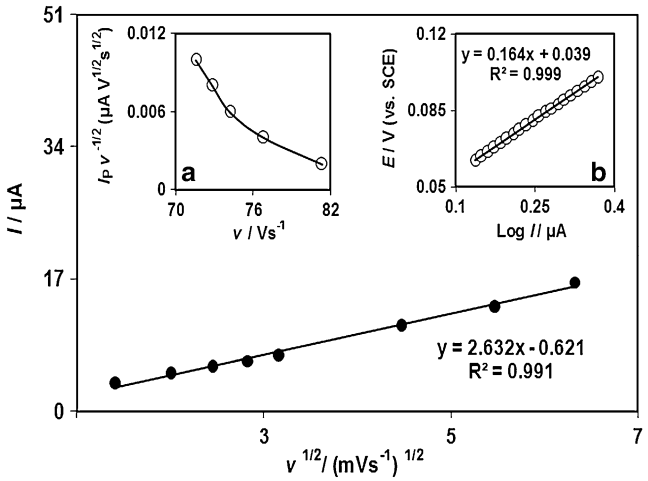

Fig. 3 Variation of the electrocatalytic peak current (I_p) with the square root of scan rate. **a** Variation of the normalized current ($I_p/v^{1/2}$) with scan rate. **b** Tafel plot derived from the rising part of voltammogram recorded at a scan rate 20 mV s^{-1}

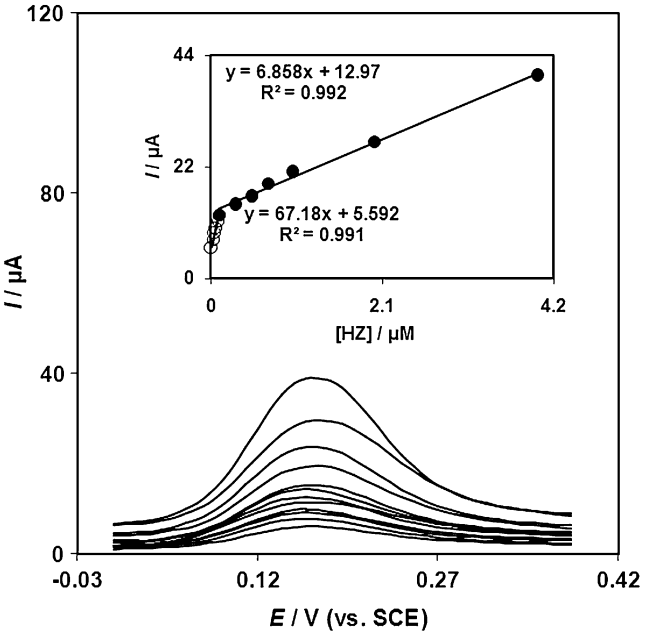

Fig. 5 **a** Differential pulse voltammograms of the DHBPDTNMCPE in 0.1-M PBS (pH 8.0) containing different concentrations of HZ, from inner to outer, correspond to 0.01, 0.03, 0.05, 0.07, 0.09 , 0.10, 0.30, 0.50, 0.70, 1.00, 2.00, and 4.00 µM of HZ. Plot of the peak currents as a function of concentration of HZ in two linear ranges of 0.01–0.10 and 0.10–4.00 µM

concentration of HZ employed. The slopes of the resulting straight lines were plotted versus the HZ concentrations (Fig. 4a). The value of the D was found to be 5.81×10^{-6} cm^2 s^{-1}. This value is comparable to values reported by other researchers for the electrocatalytic oxidation of HZ at the surface of chemically modified electrodes by other mediators previously (Table 1).

Chronoamperometry can also be employed to evaluate the catalytic rate constant (k_h) for the reaction between HZ and DHBPDTNMCPE according to the method of Galus [42]:

$$I_C/I_L = \pi^{1/2}\gamma^{1/2} = \pi^{1/2}(kC_bt)^{1/2} \quad (2)$$

where t is the time elapsed and C_b is the bulk concentration of HZ. The above equation can be used to calculate the rate constant of the catalytic process k_h. Based on the slope of the I_C/I_L versus $t^{1/2}$ plot; k_h can be obtained for a given HZ concentration. Such plot obtained from the chronoamperograms in Fig. 4 is shown in Fig. 4b. From the values of the slope, a value of k_h was found to be $k=3.65\times10^3 M^{-1}$ s^{-1} for 0.3-mM HZ. This value is comparable to values reported by other researchers for the electrocatalytic oxidation of HZ at the surface of chemically modified electrodes by other mediators previously (Table 1).

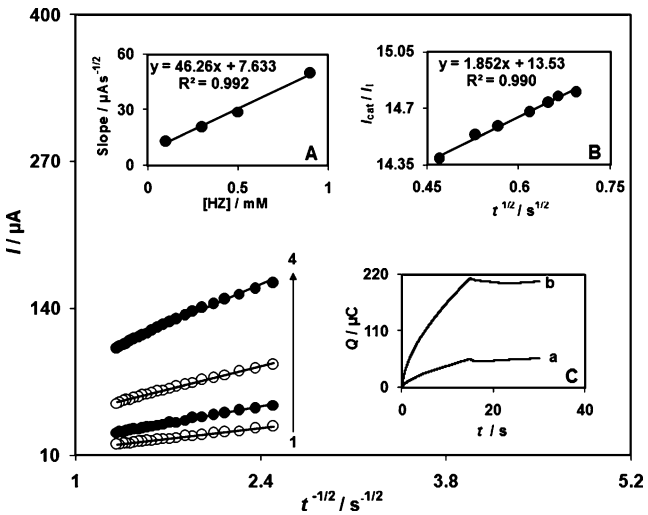

Fig. 4 Plots of I vs. $t^{-1/2}$ obtained from chronoamperograms. The numbers *1–4* correspond to 0.1, 0.3, 0.5, and 0.9 mM HZ, respectively. **a** Plot of the slope of the straight lines against the HZ concentration. **b** Dependence of I_{cat}/I_l on $t^{1/2}$ derived from the data of chronoamperogram of 0.3-mM HZ. **c** DHBPDTNMCPE chronocoulograms in the absence (**a**) and presence (**b**) of HZ

Table 2 Determination of HZ in water samples

Sample	Sample No.	Added (µM)	Found (µM)	Recovery (%)	RSD (%)
Drinking water	1	0.50	0.49	98.0	3.0
	2	1.00	1.06	106.0	1.9
River water	1	0.50	0.51	102.0	0.41
	2	1.00	0.99	99.0	2.6
Tap water	1	0.50	0.51	102.0	1.7
	2	1.00	0.99	99.0	2.0

Furthermore, double-potential step chronocoloumetry, as well as other electrochemical methods, was employed for the investigation of electrode processes at a DHBPDTNMCPE. Forward and backward potential step chronocoloumetry on the modified electrode in a blank buffer solution showed symmetrical chronocolougrams. These had about an equal charge consumed for both oxidation and reduction of the redox system in the DHBPDTNMCPE. However, in the presence of HZ, the charge value associated with forward chronocoloumetry was significantly greater than that observed for backward chronocoloumetry. This behavior is typical of that expected for electrocatalysis at chemically modified electrodes [41].

Calibration plot and limit of detection

Differential pulse voltammetry was used to determine the concentration of HZ. Voltammograms clearly show that the plot of peak current versus HZ concentration is constituted of two linear segments with different slopes (slope 67.18 μA μM^{-1} for first linear segment and 6.858 μA μM^{-1} for second linear segment), corresponding to two different ranges of substrate concentration, 0.01 to 0.10 μM for the first linear segment and 0.10 to 4.00 μM for the second linear segment (Fig. 5). The decrease of sensitivity (slope) in the second linear range is likely to be due to kinetic limitation. The detection limit (3σ) for HZ in the lower range region was found to be 9.15 nM (Table 1).

Determination of HZ in real samples

To evaluate the applicability of the proposed method to real samples, it was applied to the determination of HZ in water samples. The samples tested were found to be free from HZ, and thus, synthetic samples were prepared by adding known amounts of HZ to water samples. The results are given in Table 2.

Conclusions

This work describes the construction of a chemically modified carbon paste electrode by the incorporation of DHBPD and TiO_2 nanoparticles. Electrochemical studies show that the oxidation of HZ is catalyzed at pH 8.0. Furthermore, the mediated oxidation peak current of HZ at the surface of DHBPDTNMCPE was used for voltammetric determination of HZ in an aqueous solution.

High sensitivity and a low detection limit, together with the easy preparation and regeneration of the electrode surface, make the system discussed above useful in the construction of simple devices for the determination of HZ. Finally, the electrocatalytic oxidation of HZ at the surface of this modified electrode can be employed as a new method for the voltammetric determination of HZ in real samples.

Acknowledgments The authors wish to thank Nima Taghavinia, Yazd University Research Council and IUT Research Council and Excellence in Sensors for financial support of this research.

References

1. Welch CM, Compton RG (2006) Anal Bioanal Chem 384:601–619
2. Morales GR, Silva TR, Galicia L (2003) J Solid State Electrochem 7:355–360
3. Beitollahi H, Mazloum Ardakani M, Ganjipour B, Naeimi H (2008) Biosens Bioelectron 24:362–368
4. Katz E, Willner I, Wang J (2004) Electroanalysis 16:19–44
5. Mazloum Ardakani M, Talebi A, Naeimi H, Nejati Barzoky M, Taghavinia N (2009) J Solid State Electrochem 13:1433–1440
6. Schessl HW (1995) Encyclopedia of chemical technology, 4th edn. Wiley/Interscience, New York
7. US Environmental protection Agency (1999) Integrated risk information system (iris) on hydrazine/hydrazine sulfate. National Center for Environmental Assessment, Office of Research and Development, Washington
8. Budavari S, O'Neil MJ, Smith A (1989) The Merck index: an encyclopedia of chemicals, drugs and biologicals, 11th edn. Merck and Co. Inc.
9. Pingarron JM, Ortiz Hernandez I, Gonalez-Cores A, Yez-Sendeno P (2001) Anal Chim Acta 439:281–290
10. US Department of Health and Human Services (1993) Hazardous substances data bank (HDBS, online database). National Toxicology Information Program, National Library of Medicine, Bethesda, MD
11. Sitting M (1985) Handbook of toxic and hazardous chemical and carcinogens, 2nd edn. Noyes Publications, Park Ridge
12. World Health Organization (1987) Environmental Health Criteria 68: Hydrazine, Geneva, Switzerland
13. International Agency for Research on Cancer (IARC) (1974) IARC monographs on the evaluation of the carcinogenic risk of chemicals to man: some aromatic amines, hydrazine and related substances, N-nitroso compounds and miscellaneous alkylating agents, vol 4. World Health Organization, Lyon
14. Agency for Toxic Substances and Disease Registry (ATSDR) (1997) Toxicological profile for hydrazines. Public Health Service. US Department of Health and Human Services, Atlanta
15. National Institute for Occupational Safety and Health (NIOSH) (1997) Pocket guide to chemical hazards. US Department of Health and Human Services, Public Health Service, Centers for Disease Control and Prevention, Cincinnati
16. Occupational Safety and Health Administration (OSHA) (1998) Occupational Safety and Health Standards, Toxic and Hazardous Substances, Code of Federal Regulations, 29 CFR
17. Duarte JC, Luz RCS, Damos FS, Oliveira AB, Kubota LT (2007) J Solid State Electrochem 11:631–638
18. Yang M, Li HL (2001) Talanta 55:479–484
19. Mori M, Tanaka K, Xu Q, Ikedo M, Taoda H, Hu W (2004) J Chromatogr A 1039:135–139
20. Afkhami A, Zarei AR (2004) Talanta 62:559–565
21. Ensafi AA, Naderi B (1997) Microchem J 56:269–272
22. Safavi A, Karimi MA (2002) Talanta 58:785–792
23. Beitollahi H, Mazloum Ardakani M, Naeimi H, Ganjipour B (2009) J Solid State Electrochem 13:353–363

24. Mazloum-Ardakani M, Beitollahi H, Sheikh Mohseni MA, Benvidi A, Naeimi H, Nejati-Barzoki M, Taghavinia N (2010) Colloids, Surfaces B: Biointerfaces 76:82–87
25. Abbaspour A, Shamsipur M, Siroueinejad A, Kia R, Raithby PR (2009) Electrochim Acta 54:2916–2923
26. Zhenga L, Songa JF (2009) Talanta 79:319–326
27. Abbaspour A (2009) J Electroanal Chem 631:52–57
28. Zheng L, Song JF (2009) Sens Actuators B 135:650–655
29. Quintino MSM, Araki K, Toma HE, Angnes L (2008) Talanta 74:730–735
30. Richard Prabakar SJ, Sriman Narayanan S (2008) J Electroanal Chem 617:111–120
31. Ojani R, Raoof JB, Norouzi B (2008) Electroanalysis 20:1378–1382
32. Nassef HM, Radi AE, O'Sullivan CK (2006) J Electroanal Chem 592:139–146
33. Li J, Lin X (2007) Sens Actuators B 126:527–535
34. Abbaspour A, Kamyabi MA (2005) J Electroanal Chem 576:73–83
35. Raoof JB, Ojani R, Ramine M (2007) Electroanalysis 19:597–603
36. Zheng J, Sheng Q, Li L, Shen Y (2007) J Electroanal Chem 611:155–161
37. Jayasri D (2007) Sriman Narayanan S. J Hazard Mater 144:348–354
38. Wang G, Gu A, Wang W, Wei Y, Wu J, Wang G, Zhang X, Fang B (2009) Electrochem Commun 11:631–634
39. Mazloum Ardakani M, Ebrahimi karami P, Rahimi P, Zare HR, Naeimi H (2007) Electrochim Acta 52:6118–6124
40. Laviron E (1979) J Electroanal Chem 101:19–28
41. Bard AJ, Faulkner LR (2001) Electrochemical methods: fundamentals and applications, 2nd edn. Wiley, New York
42. Galus Z (1976) Fundamentals of electrochemical analysis. Ellis Horwood, New York